

# Mott Transition in an Anyon Gas

Wei Chen

*Department of Physics, University of British Columbia*

*Vancouver, B.C., Canada V6T 1Z1*

Matthew P.A. Fisher

*IBM Research, TJ Watson Research Center*

*PO Box 218, Yorktown Heights, NY 10598*

Yong-Shi Wu

*Center for Theoretical Physics, MIT, Cambridge, MA 02139*

*and Department of Physics, University of Utah*

*Salt Lake City, UT 84112*

We introduce and analyze a lattice model of anyons in a periodic potential and an external magnetic field which exhibits a transition from a Mott insulator to a quantum Hall fluid. The transition is characterized by the anyon statistics,  $\alpha$ , which can vary between Fermions,  $\alpha = 0$ , and Bosons,  $\alpha = 1$ . For bosons the transition is in the universality class of the classical three-dimensional XY model. Near the Fermion limit, the transition is described by a massless 2+1 Dirac theory coupled to a Chern-Simons gauge field. Analytic calculations perturbative in  $\alpha$ , and also a large N-expansion, show that due to gauge fluctuations, the critical properties of the transition are dependent on the anyon statistics. Comparison with previous calculations at and near the Boson limit, strongly suggest that our lattice model exhibits a fixed line of critical points, with universal critical properties which vary continuously and monotonically as one passes from Fermions to Bosons. Possible relevance to experi-

ments on the transitions between plateaus in the fractional quantum Hall effect and the magnetic field-tuned superconductor-insulator transition are briefly discussed.

PACS numbers: 71.30.+h 73.40.Hm 74.20.Kk

## I. INTRODUCTION

A very powerful approach for treating strongly correlated quantum models in two-dimensions has been to transform the statistics of the particles by attaching statistical flux tubes [1]. In this way, a fermion model can formally be transformed into a boson model and vice versa. Moreover, models describing particles with fractional statistics (anyons) can be mapped either way, into a fermion or a boson model. This mapping is usually accompanied by a flux smearing ‘mean field’ treatment, originally introduced by Fetter, Laughlin and Hanna [2]. In this mean field approach the statistical flux tubes are ‘detached’ from the particles and smeared uniformly in space. Taken together with the above mapping, this mean field approach effectively ‘trades in’ statistics for an external magnetic field! This approach serves as the key ingredient in various recent theories of the quantum Hall effect: For example the so-called Ginzburg-Landau approaches [3–5] which focus on an underlying Bose condensation, the hierarchical construction due to Jain [6,7] which relates integer and fractional Hall states, and most recently to theories of the half-filled Landau level [8] as a pseudo-fermi liquid. It has also recently been applied in attempt [9] to relate the continuous transitions between plateaus in the fractional Hall effect to the transition between plateaus in the integer effect.

It is generally believed that this flux-smearing mean field approximation should be legitimate when the mean field state is an incompressible fluid with a gap, such as a quantum Hall fluid. Indeed, various numerical exact diagonalizations [10] on small systems appear to confirm this belief. However, when the reference state is gapless, as for example at a transition between plateaus in the quantum Hall effect or in the fermi-liquid theories of the half-filled Landau level, the approximation is much more highly suspect. In particular various conclusions arrived at in Ref. [9] which relate detailed critical properties at transitions between different quantum Hall plateaus are worth detailed scrutiny.

The purpose of the present paper is to introduce the simplest possible anyon model which exhibits a continuous phase transition, and analyze in detail the universal critical properties near and at the transition. The model is characterized by the statistics of the

particles, which can be tuned continuously from Bose to Fermi. The particles are subject to a periodic potential with a period commensurate with the particle's density, corresponding to one particle per unit cell. Moreover, the model includes an external magnetic field, taken as zero in the boson limit, one flux quantum per particle in the fermion limit, and proportional to the statistics in the anyon case. In this way a 'mean-field' treatment of the model, as described above, would result in behavior fully independent of the particle's statistics. Controlled calculations of the actual critical properties then allow for a direct check on the validity of the mean-field approach.

In the boson limit, the model exhibits a Mott-insulator to superfluid transition which is in the universality class of the classical 3D XY model [11]. Critical properties can be extracted via Monte Carlo simulations or  $1/N$  expansions [12]. As we show below, in the Fermion limit the model is soluble and exhibits a 'gap-closing' transition between a band-insulator and an integer quantum Hall state. We analyze the critical properties in this case, which are described by a massless 2+1 Dirac equation, and find that they are most certainly different from the 3D XY model, which reveals the inadequacies of the 'mean-field' approximation.

For anyon statistics the model exhibits a transition between a Mott-insulator and a quantum Hall fluid. Can the critical properties be extracted for this anyonic Mott transition? As shown recently by Wen and Wu [13], it is possible to perform a renormalization group (RG) calculation perturbative in deviations of the particle's statistics from the bosonic point. Within a controlled  $1/N$  expansion they find that the critical properties vary continuously with the particle statistics! In RG terminology they have found a 'fixed line' parameterized by the particle's statistics. In this paper we perform a similar perturbative analysis expanding around the Fermi end, described by the Dirac equation. We likewise find that the critical exponents and other universal properties vary continuously with statistics. Again, this statistics-dependence is shown to originate from gauge-field fluctuations near the critical point. Moreover the sign of our perturbative results for the critical exponents near the Fermion point, suggest that the exponents vary monotonically upon moving along the fixed line between the Fermion and Boson transitions. We suspect that this might be a generic

feature of quantum phase transitions involving fractional statistics particles. This would imply that the leading perturbative corrections to the flux-smearing mean field treatment approach monotonically the exact behavior.

The dependence of the detailed critical properties on the statistics of the underlying particles in our model system, strongly suggests that, in contrast to recent speculations [9], the phase transition between integer plateaus in the quantum Hall effect is not in the same universality class as that between fractional plateaus. Indeed, in view of our results, it would be much more natural to argue that the exponents will depend on the statistics of the condensing quasiparticles, which of course depend on which two fractions the transition is between. However since both disorder and long-ranged Coulomb interactions are relevant perturbations at the Mott transition studied here, we cannot make any definitive statements about the universality class appropriate to experimental quantum Hall phase transitions.

The paper is organized as follows. In Section II we introduce the lattice anyon model, and discuss the continuum limit, with special emphasis on the fermion limit. The resulting critical theory is a massless 2+1 Dirac equation coupled to a Chern-Simons term. Section III is devoted to a detailed RG analysis of this fermionic Chern-Simons theory, perturbative in deviations of the statistics away from Fermi, as well as in a large N limit. In addition to the critical exponents  $\nu$  and  $\eta$  we calculate the universal Hall and longitudinal conductivities. Finally, Section IV is a discussion section with emphasis on possible relevance to experimental systems.

## II. THE MODEL

In this Section we introduce our lattice anyon model, and in the fermion case extract the appropriate continuum limit.

The Hamiltonian we study is defined for convenience in terms of spinless fermion operators:

$$H = - \sum_{ij} (t_{ij} c_i^\dagger c_j + h.c.) + m \sum_j s_j c_j^\dagger c_j . \quad (1)$$

where the fermion operators satisfy the usual anticommutation relations:

$$\{c_i, c_j^\dagger\} = \delta_{ij} . \quad (2)$$

Here  $i$  and  $j$  label sites of a square lattice,  $t_{ij}$  is a hopping matrix element and  $s_j = +1$  for sites of one sub-lattice and  $-1$  on the other sub-lattice. The second term in the Hamiltonian is thus a staggered potential with strength  $m$ . We restrict attention exclusively to half-filling, so that the number of particles equals the number of sites on either of the two sub-lattices.

An applied magnetic field,  $B$ , and flux tubes attached to the fermions both enter via a gauge field:  $t_{ij} = |t_{ij}|e^{iA_{ij}}$ . For later convenience we take the hopping strength  $|t_{ij}|$  to be equal to  $t$  for nearest neighbor sites,  $t'/4$  for next nearest neighbors and zero otherwise. The gauge field is chosen so that

$$\nabla \times A = B + \alpha \rho , \quad (3)$$

where  $\nabla \times A$  denotes a lattice curl, that is an oriented sum of  $A_{ij}$  around plaquettes, and  $B$  is a uniform external field in units of a flux quantum,  $h/e$ , per elementary square of the lattice. Here  $\rho$ , which is an operator, denotes the particle density so that Eq.(3) must be thus taken as a constraint. The statistics parameter  $\alpha$  gives the strength of the statistical flux tubes which are thereby attached to each particle. With  $\alpha = 1$  the particles are transmuted into bosons, whereas anyons correspond to  $\alpha$  between zero and 1. Finally, to fully specify the model we choose the external field as  $B = (1 - \alpha)/2$ , so that at half-filling in a flux-smearing mean-field treatment the Hamiltonian reduces to bosons in zero field, for all  $\alpha$ .

Notice that the model has been constructed so that in the boson limit ( $\alpha = 1$ ) it is formally equivalent to a lattice model of hard core bosons in zero magnetic field. Moreover, at half-filling the boson density is commensurate with the period of the staggered potential. This boson model is expected to undergo a Mott-insulator to superfluid transition [11] as the ratio of the kinetic energy ( $t, t'$ ) to the staggered potential ( $m$ ) is varied. This zero temperature quantum transition is expected to be in the universality class of the classical 3-dimensional XY model. The appropriate coarse-grained continuum theory to describe the behavior near the transition is then simply a  $\phi^4$  complex scalar field theory.

For  $\alpha$  near 1, the model corresponds to anyons with statistics ‘close’ to bosonic, in a weak magnetic field. In this case the model is expected to exhibit a transition from a Mott-insulator to a gaped quantum Hall fluid. The transition can be studied by adding a Chern-Simons term to the scalar field theory, which attaches  $(1 - \alpha)$  flux tubes to each boson. The corresponding critical behavior has been studied in a recent large- $N$  approach [13], and the exponents found to vary continuously with  $\alpha$ .

When  $\alpha = 0$  the Hamiltonian is simply that of non-interacting spinless fermions in a magnetic field, and can be solved by straightforward diagonalization. Specifically, with  $1/2$  flux per square and the staggered potential the unit cell has four sites [14], as sketched in Fig. 1. Extracting the band structure thus involves diagonalizing a 4 by 4 matrix. Doing so reveals that generally there are two bands, symmetric about zero energy (half-filling), with a band gap about the origin. Depending on the relative sizes of  $t'$  and  $m$  the bands can be either ‘Landau levels’, which contribute a Hall conductance, or conventional insulating band with no Hall effect [15]. Of interest to us is the transition between these two phases, where the band gap closes. (Across the transition the Hall conductance jumps from unity to zero, in units of  $e^2/h$  with  $e$  the electric charge of the fermion.) The band structure reveals that the gap closes at a single point in crystal momentum ( $k$ -) space. By focusing on values of  $k$  near this point, we now construct a continuum field theory for the behavior near the transition.

To this end, we choose an explicit gauge for the  $A_{ij}$ , which is shown in Figure (1). Moreover, we put  $t=1$  and take  $t'$  and  $m$  much smaller than 1. In this limit the band gap vanishes when  $t' = m$  and occurs at  $(\pi, \pi)$  in the Brouillon zone. Upon linearizing the momentum about this point the Hamiltonian can be cast in the form:

$$H = \int_p \sum_{a,b=1}^4 c_a^\dagger(p) H_{ab}(p) c_b(p), \quad (4)$$

where  $c_a(p)$  denotes the Fourier transform of the electron operators on the ‘ $a$ ’ sites (see Fig. 1) at momentum  $(\pi, \pi) + p$ . The 4 by 4 matrix  $H_{ab}$  can be written [16]:

$$H_{ab}(p) = (p_y \sigma_y - m \sigma_z) \otimes 1 + (p_x \sigma_x + t' \sigma_z) \otimes \tau_y, \quad (5)$$

where  $\sigma_\mu$  and  $\tau_\mu$  denote the usual Pauli matrices and  $\otimes$  is a direct product. Upon performing a basis rotation on  $\tau_\mu$  by 90 degrees about the x-axis, the Hamiltonian can be transformed into a 2 by 2 block diagonal form,

$$H_{ab}(p) = H_+(1 + \tau_z)/2 + H_-(1 - \tau_z)/2, \quad (6)$$

with

$$H_\pm = \pm p_x \sigma_x + p_y \sigma_y + (\pm t' - m) \sigma_z, \quad (7)$$

Notice that  $H_+$  is a two-dimensional Dirac Hamiltonian with mass,  $M = t' - m$ , which vanishes at the transition. Under  $\sigma_x \rightarrow -\sigma_x$ ,  $H_-$  is also a Dirac Hamiltonian except with mass  $t' + m$ . This mass remains non-zero when  $m = t'$ , and thus non-critical. As far as critical properties near the transition are concerned we can safely ignore the massive field and focus exclusively on the single Dirac field which goes massless. Since this theory is non-interacting we can easily extract all of the relevant critical properties (see Section 3).

When the statistics parameter  $\alpha$  is non-zero, but small, progress can be made by expanding around the fermion point (ie. the Dirac equation). The appropriate continuum theory near the transition in this case can be simply obtained from the Dirac equation by minimal coupling to the gauge field whose associated flux must be attached to the fermions. This can be achieved in the usual way by the addition of a Chern-Simons term [17] to the 2+1 Dirac Lagrangian. In the next Section we perform a renormalization group analysis on this 2+1 Dirac plus Chern-Simons theory to extract critical properties near the anyon Mott transition. Two expansions are available for calculating them: the weak ‘coupling’ expansion, in which the small parameter is  $\alpha$ , the deviation from Fermi statistics, and the  $1/N$  expansion, if one consider the case with  $N$  species of anyons.

### III. CRITICAL PROPERTIES

The quantities of primary physical interest which characterize the Mott transition are the transverse and longitudinal conductivities at the critical point, and the usual critical exponents  $\eta$  and  $\nu$ . It has recently been argued [18] that in general at zero temperature



quantum phase transitions in two spatial dimensions, the conductivity should be universal, and we indeed verify this below for the anyon Mott transition. As usual we define the exponent  $\nu$  in terms of the correlation length which diverges as  $M^{-\nu}$ , upon approaching the transition by taking the Dirac mass  $M = m - t'$  to zero. We define the exponent  $\eta$  via the decay of the two-point anyonic correlation function

$$\langle \psi^\dagger(x)\psi(0) \rangle \sim x^{-(1+\eta)}, \quad (8)$$

where  $\psi$  is the anyon field operator in either a fermionized or bosonized representation. Implicit in this definition is the assumption that the anyons are converted into Fermions or Bosons by attaching flux tubes in the Landau gauge, where the vector potential is divergence free. Notice that in the above definition of  $\eta$  we have pulled out a factor of 1, so that it coincides with the usual exponent  $\eta$  at the Boson Mott-insulator to superfluid transition [11], where the 1 is twice the canonical dimension of the boson field and  $\eta$  twice the anomalous dimension. However, as we see below, at the Fermion Mott transition the scaling dimension of the Fermi field is 1, and there is no anomalous dimension, so that in this case  $\eta = 1$ , rather than twice the anomalous dimension.

To extract critical properties near the Fermion point we employ a renormalization group (RG) analysis in the framework of continuum Euclidean field theory [19,20] by applying standard diagrammatic perturbative techniques [21].

### 1) Field Theory Approach

As shown in Section II, the long-length scale and low energy physics near the anyon Mott transition can be described by two D=2+1 Dirac fermions, one of which becomes massless at the transition, which are coupled to a Chern-Simons gauge field  $a_\mu$ . Specifically, from the Hamiltonian  $H$  in Eq. (6) and the constraint in Eq. (3), the appropriate Euclidean Lagrangian is simply

$$L = \sum_{\pm} \psi_{\pm}^\dagger [\gamma_\mu (\partial_\mu - i g a_\mu) + i M_{\pm}] \psi_{\pm} + i \frac{1}{2} \epsilon_{\mu\nu\lambda} a_\mu \partial_\nu a_\lambda. \quad (9)$$

where  $\psi_{\pm}$  are the two species of Dirac fields. Here the Dirac matrices in three dimensions are  $\gamma_\mu = i\sigma_\mu$ , with  $\sigma_\mu$  ( $\mu = 1, 2, 3$ ) Pauli matrices, so that

$$\gamma^\mu \gamma^\nu = -\delta^{\mu\nu} \mathbf{1} - \epsilon^{\mu\nu\lambda} \gamma^\lambda, \quad \mathbf{Tr}(\gamma^\mu) = 0. \quad (10)$$

We have normalized the coefficient of the Chern-Simons term, and the ‘coupling constant’  $g^2$  is essentially the anyon statistics,  $\alpha$ , measured from the fermion point:

$$g^2 = 2\pi\alpha. \quad (11)$$

A source electromagnetic field which can be used to calculate the conductivities within linear response is minimally coupled to the Dirac fields in the usual way. It is worth emphasizing that the sign of the Chern-Simons term in the Lagrangian (9) must be chosen correctly in order that the flux tubes attached to the particles are in the opposite direction to the external physical magnetic field.

The phase transition between the quantum Hall phase and the Mott insulator occurs when one of the Dirac masses, say  $M = M_+$ , passes through zero. Before discussing the associated critical properties it is instructive to first recover the expected behavior of the two phases from the above Lagrangian. Provided we put in an ultraviolet cutoff, which is appropriate for the original lattice theory, when both masses are non-zero straightforward perturbation theory in powers of  $g^2$  is convergent. Consider, for example, the fermion ‘polarization tensor’, defined as the Fermion current-current correlation function, which we denote as  $\Pi_{\mu\nu}(p)$ . Current conservation (or gauge invariance) implies that the polarization tensor is always transverse:  $p_\mu \Pi_{\mu\nu}(p) = 0$ . Such a tensor in  $D = 3$  can be decomposed into an even and odd part:

$$\Pi_{\mu\nu}(p) = \Pi_e(p) p (\delta_{\mu\nu} - \frac{p_\mu p_\nu}{p^2}) + \Pi_o(p) \epsilon_{\mu\nu\lambda} p_\lambda. \quad (12)$$

where we have used the notation  $p = |p|$ . From standard linear response theory, the two parts are related to the Fermion longitudinal and transverse conductances, in units of  $e^2/h$  with  $e$  the charge, by

$$\sigma_{F,xx} = -\frac{1}{\alpha} \Pi_e(0), \quad \sigma_{F,xy} = -\frac{1}{\alpha} \Pi_o(0). \quad (13)$$

The conductance of the anyons has an additional contribution coming from the attached flux tubes. Formally this is due to the difference between the anyon current operator,

$\gamma_\mu \psi^\dagger (\partial_\mu - i g a_\mu) \psi$ , which couples to the physical electromagnetic field, and the Fermion current operator:  $\gamma_\mu \psi^\dagger \partial_\mu \psi$ . (see Fig. 2). As can be easily shown (see e.g. [13]), the anyon resistivity tensor,  $\rho_{ij}$ , is simply related to the fermionic resistivity tensor via:

$$\rho_{ij} = \rho_{F,ij} - \epsilon_{ij} \alpha. \quad (14)$$

Previously there has been an intense effort in analyzing the Chern-Simons gauge theory coupled to a Dirac field in perturbation theory employing standard diagrammatic techniques [22,23,25–30,32]. Specifically, for a massive Dirac field it has been shown that the one-loop diagram in Fig. 3a contributes a finite contribution to the odd part of the Fermion polarization,  $\Pi_o^{(1)}(p = 0) = +(\alpha/2) \text{sgn}(M_\pm)$ . Notice the dependence on the sign of the Dirac mass. Moreover it has been proved [23,26] that in the massive theory there are no additional non-zero corrections to the Fermion polarization,  $\Pi_{e,o}(0)$ , to all orders in  $\alpha$ . Thus away from the Mott transition the Fermion conductivity tensor which follows from Eqn. 13 is given by

$$\sigma_{F,ij} = -\frac{1}{2} \epsilon_{ij} \sum_{\pm} \text{sgn}(M_\pm). \quad (15)$$

In the Mott insulating phase, where the two masses have different signs, the conductivity tensor vanishes as expected, whereas in the Quantum Hall effect phase one has simply  $\sigma_{F,ij} = -\epsilon_{ij}$ . The total anyon resistivity tensor in the quantum Hall phase is then  $\rho_{ij} = \epsilon_{ij}(1 - \alpha)$ . Notice that when  $\alpha = 1$ , which corresponds to the bosons superfluid phase (in zero magnetic field), the Hall resistivity vanishes as expected.

We now turn to the critical properties near the transition where the mass of one Dirac field,  $M = M_+$  vanishes. In the following we focus exclusively on the massless Dirac field, since the contributions from the massive field are known to all orders, as described above. Consider a renormalization group (RG) transformation for this massless field, which involves integrating over a shell of (three-)momenta  $p$  in a shell between  $\Lambda$  and  $\Lambda/b$ , with  $b > 1$ . To complete the RG we rescale the momenta by  $b$  and the fields  $\psi$  and  $a$  by  $b^{1+\gamma_\psi}$  and  $b^{1+\gamma_a}$ , respectively. The anomalous dimensions will be chosen to keep the coefficients of the

quadratic terms in the Lagrangian Eqn. (9) fixed. Power counting at the Gaussian ( $g = 0$ ) fixed point reveals that the coupling constant  $g$  is indeed dimensionless. A straightforward perturbative renormalization group can then be carried out using standard methods. As defined above in Equation (8) the critical exponents  $\eta$  and  $\nu$  are related to the anomalous dimension of the massless Fermion field,  $\psi$ , and that of the composite operator  $\bar{\psi}\psi$ , which we denote by  $\gamma_{\bar{\psi}\psi}$  [19,20]:

$$\eta = 1 + 2\gamma_{\psi} , \quad \nu^{-1} = 1 - \gamma_{\bar{\psi}\psi} \quad (16)$$

It can be easily shown ([26]) at one-loop order that the beta-function,  $\beta(g) = -dg/d\ln(b) = O(g^5)$ , vanishes. Indeed it has been suggested [26] and shown explicitly to second order, that the beta-function vanishes identically:

$$\beta(g) = 0 . \quad (17)$$

This implies that there is a line of fixed points or critical points, parametrized by the anyon statistics  $\alpha$ ! Unfortunately all of the anomalous dimensions vanish at one-loop order, so it is necessary to go to second order to evaluate the leading non-trivial corrections to the exponents. In addition to the critical exponents, the universal anyon conductivity at the critical point is of interest. As first emphasized by Semenoff, Sodano and Wu [26], in contrast to the massive theory, in the massless theory there is a non-vanishing two loop contribution to the conductivity. Indeed, the exact value of this correction was obtained subsequently by Chen [29,30]. In the following we will give a unified description of the two-loop perturbative results for the critical properties of the model (9) in the context of the anyon Mott transition, together with some new calculations when the quantities of interest are not available in the literature.

## 2) Weak-Coupling Expansion

In this subsection we carry out a two-loop perturbation expansion in powers of the coupling constant  $g^2$  to extract critical exponents and the universal conductivity. We take the Landau gauge, by adding a gauge fixing term,  $(1/2\lambda)(\partial_{\mu}a_{\mu})^2$ , to the Lagrangian (9)

and then take the limit  $\lambda \rightarrow 0$  in the resulting propagator for the gauge field. With the normalization chosen as shown in eq.(9) the appropriate Feynman rules for the massless Dirac field in the Landau gauge are

$$\text{the fermion propagator} \quad S_0(p) = \frac{1}{i \not{p}} , \quad (18)$$

$$\text{the gauge propagator} \quad G_0^{\mu\nu}(p) = -\frac{\epsilon^{\mu\nu\lambda} p^\lambda}{p^2} , \quad (19)$$

$$\text{the interaction vertex} \quad \Gamma_0^\mu(p) = ig\gamma^\mu . \quad (20)$$

The advantage of the Landau gauge is that no infra-red divergences would appear perturbatively in this gauge [22,26–28].

Since we require a two-loop calculation, rather than regularizing in the ultraviolet with a finite momentum cutoff,  $\Lambda \approx 1/a$ , it is more convenient to regularize by dimensional reduction and also employ a minimal subtraction method. In this approach, which was first suggested and extensively used in Refs. [27,28] for the  $D = 3$  Chern-Simons gauge theory, all momentum integrals in the loop-expansion are continued to general dimension  $D$ :

$$\int \frac{d^3 k}{(2\pi)^3} \rightarrow \mu^{3-D} \int \frac{d^D k}{(2\pi)^D} , \quad (21)$$

where, in order to balance the dimension, one must introduce a parameter  $\mu$  which has dimension of mass. All vector, tensor and spinor quantities and in particular the symbol  $\epsilon^{\mu\nu\lambda}$  that appears in the original Feynman integrands, though, are always treated as if they were formally three dimensional. This implies that we will use the identities

$$\delta^{\mu\mu} = 3 , \quad (22)$$

$$\epsilon^{\mu\nu\lambda} \epsilon^{\mu\tau\eta} = \delta^{\nu\tau} \delta^{\lambda\eta} - \delta^{\nu\eta} \delta^{\lambda\tau} \quad (23)$$

before performing any momentum integrals. Finally, we adopt a minimal subtraction method for renormalization, by removing the simple poles in  $\epsilon \equiv 3 - D$  [34] and setting all higher-order poles to be zero. The parameter  $\mu$  we introduced in Eqn. (21) represents, as usual, the “renormalization point” in the minimal subtraction approach. In all cases that have been checked [27–30], including pure Chern-Simons (Abelian or non-Abelian) gauge theory,

coupled or not to massless or massive boson or Fermion matter fields, this approach to regularization and renormalization has been shown to respect both gauge invariance and Ward identities, at least up to two loops.

We consider first the universal conductances at the critical point ( $M = 0$ ), focussing exclusively on the contribution from the massless Dirac field. (The contribution from the massive field is given in Eqn. (15).) The one-loop polarization tensor  $\Pi_{\mu\nu}^{(0)}(p)$ , due to the (massless) fermion bubble (Fig. 3a), is purely symmetric in the indices  $\mu$  and  $\nu$  and given by:

$$\Pi_e^{(1)}(p) = -\frac{g^2}{16}, \quad \Pi_o^{(1)}(p) = 0. \quad (24)$$

Thus upon using Eqn. (11) and (13), to leading (zero'th) order in  $\alpha$ , the total Fermion (and anyon) conductivity at the Mott transition is given by  $\sigma_{F,xy} = 1/2$ , coming solely from the massive Dirac field, and  $\sigma_{F,xx} = \pi/8$ . It is interesting that this value is precisely equal to the value of  $\sigma_{xx}$  obtained at the Boson Mott-insulator to superfluid transition within a large-N limit [18].

The leading (linear) corrections in  $\alpha$  come from the three two-loop diagrams, shown in Fig. 4, which contribute to the polarization tensor. It turns out that all three contributions are antisymmetric in the indices  $\mu$  and  $\nu$ , namely:

$$\Pi_{\mu\nu}^{(2)}(p) = \epsilon_{\mu\nu\lambda} p_\lambda \Pi_o^{(2)}(p). \quad (25)$$

This implies that there is no correction at this order to the longitudinal Fermion conductivity,  $\sigma_{F,xx}$ . The contribution to the Hall conductivity can be obtained by contracting each diagram in Fig. 4 with  $\frac{1}{2p^2}\epsilon^{\mu\nu\lambda}p^\lambda$  and performing a trace over the Dirac spinor-components, which gives:

$$\Pi_{o(a+b)}^{(2)} = 8\frac{g^4}{p^2}\mu^{6-D'-D} \int \frac{d^{D'}k}{(2\pi)^{D'}} \frac{d^Dq}{(2\pi)^D} \frac{p \cdot (k+p)q \cdot (q+k)}{k^2(k+p)^2(k+q)^2q^2}, \quad (26)$$

$$\Pi_{o(c)}^{(2)} = 2\frac{g^4}{p^2}\mu^{6-D'-D} \int \frac{d^{D'}k}{(2\pi)^{D'}} \frac{d^Dq}{(2\pi)^D} \frac{F(q,k,p)}{k^2(k+p)^2(k+q)^2(k+q+p)^2q^2}, \quad (27)$$

$$F(q,k,p) = q^2[3k^2p^2 - 2(k \cdot p)^2 + (k \cdot p)p^2 - (k \cdot p)(q \cdot p) + (k \cdot q)p^2] \\ - k^2(q \cdot p)^2 + (k \cdot q)[2(k \cdot p)(q \cdot p) - 2(k \cdot q)p^2 - (q \cdot p)p^2]. \quad (28)$$

Since the integrals over  $k$  in Eqs. (26, 27) are convergent directly in  $D' = 3$  dimensions, we perform them there to obtain

$$\Pi_{o(a+b)}^{(2)} = \frac{g^4}{4p^2} \mu^{(3-D)} \int \frac{d^D q}{(2\pi)^D} \left[ \frac{p}{q|q+p|} - \frac{p \cdot (q+p)}{q^2|q+p|} \right], \quad (29)$$

$$\Pi_{o(c)}^{(2)} = \frac{g^4}{4p^2} \mu^{(3-D)} \int \frac{d^D q}{(2\pi)^D} \left[ \frac{q \cdot p |p|}{q^2(q+p)^2} + \frac{p \cdot (q+p)}{q^2|q+p|} \right]. \quad (30)$$

The second terms in Eqs. (29, 30) are each logarithmically divergent in  $D = 3$  but cancel one another exactly. The remaining finite contribution in  $D = 3$  is finally:

$$\Pi_o^{(2)}(p) = \Pi_o^{(2)}(0) = \Pi_{o(a+b)}^{(2)} + \Pi_{o(c)}^{(2)} = -\frac{g^4}{16\pi^2} \left(1 + \frac{\pi^2}{4}\right). \quad (31)$$

This result was obtained previously in Ref. [30] and, up to an overall sign, independently in Ref. [31] (where the convention is that there is no imaginary unit in front of the Chern-Simons term).

Upon inserting Eqn.(24) and (31) into (13) we obtain the final result for the Fermion conductivity at the anyonic Mott transition, valid up to first order in  $\alpha$ :

$$\sigma_{F,xx} = \frac{\pi}{8}, \quad (32)$$

$$\sigma_{F,xy} = -\frac{1}{2} + \frac{1}{4} \left(1 + \frac{\pi^2}{4}\right) \alpha. \quad (33)$$

The contribution of  $-1/2$  at  $\alpha = 0$  comes from the second Dirac field which remains massive at the transition. The anyon conductivity follows by inverting to get the Fermion resistivity, and then using Eq. (14). Note again that at this order there is no correction to the longitudinal Fermion conductivity. An advantage of the  $1/N$  method, which we describe in the next section, is that non-trivial corrections to  $\sigma_{F,xx}$  do appear at leading order in  $1/N$ .

To obtain the critical exponent  $\eta$ , let us consider the fermion self-energy  $\Sigma(p)$ , defined as usual via the full Fermion propagator:

$$S(p)^{-1} = S_0(p)^{-1} - \Sigma(p). \quad (34)$$

At one-loop order it is given by the diagram in Fig. 3b:

$$\Sigma^{(1)}(p) = -i\frac{g^2}{8}p. \quad (35)$$

The two-loop fermion self-energy diagrams are given in Fig. 5. In Ref. [28] these diagrams have been evaluated to obtain:

$$\Sigma^{(2)}(p) = i \not{p} \left\{ \frac{g^4}{24\pi^2} \left[ \frac{2}{3-D} + \ln\left(\frac{\mu^2}{p^2}\right) \right] + \text{finite} \right\}. \quad (36)$$

Notice that at this order the renormalized mass remains zero,  $\Delta M = \Sigma(p=0) = 0$ , implying that conformal invariance survives quantum fluctuations at the transition point  $M = 0$ . The Fermion wave function renormalization constant is extracted to be

$$Z_\psi^{-1} = \left[ \frac{\partial S^{-1}(p)}{\partial(i \not{p})} \right]_{p=0} = 1 - \frac{g^4}{12\pi^2} \frac{1}{3-D}. \quad (37)$$

One can thereby obtain the anomalous dimension  $\gamma_\psi$  of the massless anyon field up to second order:

$$\gamma_\psi = -\frac{1}{2} \frac{\partial Z_\psi}{\partial(1/\epsilon)} = -\frac{g^4}{24\pi^2}. \quad (38)$$

Finally let us consider the renormalization of the composite operator  $\bar{\psi}\psi$ , from which we can extract the critical exponent  $\nu$ . We insert this composite operator into one- and two-loop fermion self-energy diagrams, as shown in Figs. 4 and 5, with the insertion represented by a cross. To simplify the calculation, the external momentum associated with the  $\bar{\psi}\psi$  insertion is taken to be zero. We start with the one-loop diagrams, i.e. Fig. 6a, 6b, and 6c. Within our regularization scheme these diagrams are finite in  $D = 3$ :

$$(6a) = (6b) = -i\frac{g^2}{8} \frac{\epsilon^{\mu\nu\lambda} p^\lambda}{p}, \quad (39)$$

$$(6c) = -\frac{g^2}{8} \frac{\not{p}}{p}. \quad (40)$$

so that the anomalous dimension of the operator  $\bar{\psi}\psi$  indeed vanishes at one-loop order.

However, the two-loop diagrams in Fig. 7 have logarithmic divergences. After lengthy but straightforward calculations we have (up to finite contributions which do not contribute to the anomalous dimension)



$$\begin{aligned}
(7a_1) &= \frac{g^4}{8} \mu^{3-D} \int \frac{d^D k}{(2\pi)^D} \frac{1}{k(k+p)^2}, \\
(7a_2) + (7a_3) &= \frac{g^4}{2} \mu^{3-D} \int \frac{d^D k}{(2\pi)^D} \frac{1}{k(k+p)^2}, \\
(7b_1) &= -\frac{g^4}{4} \mu^{3-D} \int \frac{d^D k}{(2\pi)^D} \frac{1}{k(k+p)^2}, \\
(7b_2) + (7b_3) &= \frac{g^4}{2} \mu^{3-D} \int \frac{d^D k}{(2\pi)^D} \frac{1}{k(k+p)^2}.
\end{aligned} \tag{41}$$

The calculation of Figs.  $7c_1 - 7c_3$  is a bit more complicated, because of the Dirac matrices. However, since we are only interested in the contribution proportional to the  $2 \times 2$  unit matrix  $\mathbf{1}$ , it is sufficient to perform a trace over the product of Dirac matrices to obtain (again up to finite parts)

$$\begin{aligned}
(7c_1) + (7c_2) + (7c_3) &= 6g^4 \mu^{6-D'-D} \int \frac{d^{D'} k}{(2\pi)^{D'}} \frac{d^D q}{(2\pi)^D} \frac{k^2 q^2 - (k \cdot q)^2}{k^2 q^2 (k+p)^2 (q+p)^2 (k+q+p)^2} \\
&= \frac{3}{8} g^4 \mu^{3-D} \int \frac{d^D q}{(2\pi)^D} \frac{1}{q^2 |q+p|},
\end{aligned} \tag{42}$$

where we have used  $q \cdot k = \frac{1}{2}[(q+k+p)^2 + p^2 - (q+p)^2 - (k+p)^2]$ .

Finally, upon using the formula

$$\mu^{3-D} \int \frac{d^D k}{(2\pi)^D} \frac{1}{k(k+p)^2} = \frac{1}{4\pi^2} \left[ \frac{2}{3-D} + \ln\left(\frac{\mu^2}{p^2}\right) \right], \tag{43}$$

and putting everything together, we obtain the following divergent contribution to the Fermion self-energy with mass insertion:

$$\Gamma_{\bar{\psi}\psi}^{(2,0)} = 1 + \frac{5g^4}{16\pi^2} \left[ \frac{2}{3-D} + \ln\left(\frac{\mu^2}{p^2}\right) \right]. \tag{44}$$

Upon using the renormalization relation

$$(\Gamma_{\bar{\psi}\psi}^{(2,0)})_R = Z_\psi Z_{\bar{\psi}\psi} \Gamma_{\bar{\psi}\psi}^{(2,0)}, \tag{45}$$

and Eqs. (37), (44), we can obtain the renormalization constant and the anomalous dimension of the composite operator:

$$Z_{\bar{\psi}\psi} = 1 - \frac{17g^4}{24\pi^2} \frac{1}{3-D}, \tag{46}$$

$$\gamma_{\bar{\psi}\psi} \equiv \frac{\partial Z_{\bar{\psi}\psi}}{\partial(1/\epsilon)} = -\frac{17g^4}{24\pi^2}. \quad (47)$$

Finally, upon inserting Eqs. (38) and (47) into (16), which defines the critical exponents  $\eta$  and  $\nu$ , we find up to second order in  $\alpha$ :

$$\eta = 1 - \frac{1}{3}\alpha^2, \quad \nu^{-1} = 1 + \frac{17}{6}\alpha^2. \quad (48)$$

### 3) 1/N Expansion

In this subsection we consider a large N expansion which has the advantage of giving a non-vanishing leading correction to the Fermion longitudinal conductivity, in contrast to that found above. To this end, we consider generalizing the Lagrangian in Eqn. (9) for the massless Dirac field coupled to Chern-Simons gauge-field to include N massless Dirac fields. Once again we ignore for now the trivial contributions from the massive field. The appropriate Lagrangian is

$$L = \sum_{i=1}^N \psi_i^\dagger [\gamma_\mu (\partial_\mu - i\frac{g}{\sqrt{N}}a_\mu) + M] \psi_i + i\frac{1}{2}\epsilon_{\mu\nu\lambda} a_\mu \partial_\nu a_\lambda. \quad (49)$$

where as usual the coupling constant has been scaled by 1/N. The 1/N expansion is a formal summation of diagrams in powers of 1/N, rather than powers of  $g^2$  as in the previous section. Below we obtain the leading 1/N corrections to the conductivities at the transition and the critical exponents.

At the critical point,  $M = 0$ , the Feynman rules in the Landau gauge now read

$$S_0(p) = \frac{1}{i \not{p}}, \quad (50)$$

$$G_0^{\mu\nu}(p) = -\frac{\epsilon^{\mu\nu\lambda} p^\lambda}{p^2}, \quad (51)$$

$$\Gamma_0^\mu(p) = i\frac{g}{\sqrt{N}}\gamma^\mu. \quad (52)$$

However, in the 1/N expansion, rather than using the ‘bare’ gauge field propagator, Eq. (51), it is more convenient to first sum up the chain of Fermion bubble diagrams shown in Figure. 6, since they each contribute at the same order, namely  $\mathcal{O}(1/N^0)$ . (Each fermion loop now carries an extra factor  $N$  because of the summation over flavors, and the two

interaction vertices carry  $g^2/N$ .) Upon using Eqs. (12) and (24) to help sum up the bubbles in Fig. 8, we obtain an effective (or dressed) gauge-field propagator, denoted by a cross line in the Figures, as follows

$$G_{eff}^{\mu\nu}(p) = A \frac{\delta^{\mu\nu} p^2 - p^\mu p^\nu}{p^3} + B \frac{\epsilon^{\mu\nu\lambda} p^\lambda}{p^2}, \quad (53)$$

$$A = \frac{g^2}{16} \frac{1}{1 + (\frac{g^2}{16})^2}, \quad B = -\frac{1}{1 + (\frac{g^2}{16})^2}. \quad (54)$$

A feature of the  $1/N$  expansion in the present model is that non-trivial corrections to the critical exponents arise already at leading order (in  $1/N$ ), in contrast to the weak coupling expansion, where it was necessary to go to two-loop order to see corrections. In addition, as verified by explicit calculations below, the  $1/N$  expansion maintains conformal invariance at the transition point  $M = 0$ , at least at the leading order in  $1/N$ .

To leading order,  $\mathcal{O}(1/N)$ , the Fermion self-energy is given by the diagram in Fig. 9. We have verified that it does not shift (or renormalize) the Fermion mass from  $M = 0$ . To extract the term that is proportional to  $\not{p}$ , we perform  $-\frac{1}{2p^2} \not{p} \mathbf{Tr} \not{p}$  on the diagram in Fig. 9. Keeping only the divergent part, we thereby find

$$\Sigma(p) = i \not{p} \frac{g^2 A}{6\pi^2 N} \left[ \frac{2}{3-D} + \ln\left(\frac{\mu^2}{p^2}\right) \right]. \quad (55)$$

which gives directly the anomalous dimension:

$$\gamma_\psi = -\frac{g^2 A}{6\pi^2} \frac{1}{N}. \quad (56)$$

Upon insertion of the operator  $\bar{\psi}\psi$  into the one-loop Fermion self-energy, we have the three diagrams in Fig. 10, which up to finite parts give a contribution:

$$(10a) = 2A \frac{g^2}{N} \mu^{3-D} \int \frac{d^D k}{(2\pi)^D} \frac{1}{(k+p)^2 k}$$

$$(10b) + (10c) = -\frac{g^4}{2N} (A^2 - B^2) \mu^{3-D} \int \frac{d^D k}{(2\pi)^D} \frac{1}{(k+p)^2 k}. \quad (57)$$

Performing the loop integrals then gives

$$\Gamma_{\bar{\psi}\psi}^{(2,0)} = 1 + \left[ 2A - \frac{(A^2 - B^2)g^2}{2} \right] \frac{g^2}{4\pi^2 N} \left[ \frac{2}{3-D} + \ln\left(\frac{\mu^2}{p^2}\right) \right], \quad (58)$$

$$Z_{\bar{\psi}\psi} = 1 - \left[ \frac{8}{3}A - \frac{(A^2 - B^2)g^2}{2} \right] \frac{g^2}{2\pi^2 N} \frac{1}{3-D}, \quad (59)$$

and the anomalous dimension

$$\gamma_{\bar{\psi}\psi} = -\left[\frac{8}{3}A - \frac{(A^2 - B^2)g^2}{2}\right]\frac{g^2}{2\pi^2 N}. \quad (60)$$

Finally, upon inserting Equations (56) and (60) into (16) we obtain the leading  $1/N$  expressions for the critical exponents:

$$\eta = 1 - \frac{8}{3} \frac{\alpha^2}{64 + (\pi\alpha)^2} \frac{1}{N}, \quad (61)$$

$$\nu^{-1} = 1 + \frac{128}{3} \frac{(128 - (\pi\alpha)^2)\alpha^2}{(64 + (\pi\alpha)^2)^2} \frac{1}{N}. \quad (62)$$

Next we calculate the order  $1/N$  corrections to the conductivities at the critical point. The relevant Feynman diagrams which contribute to the Fermion polarization tensor are listed in Figs. 11 and 12. The diagram in Fig. 12 is zero by Furry's theorem, because it contains a closed Fermion loop attached to an odd number of gauge-field lines. (Essentially this is a consequence of charge-conjugation invariance, since the Chern-Simons gauge boson has odd charge parity.) Fig. 11a, 11b, and 11c are linear in  $G_{eff}^{\mu\nu}$  and therefore linear in  $\epsilon^{\mu\nu\lambda}$  and in  $(\delta^{\mu\nu} - p^\mu p^\nu / p^2)$ . Thus the odd contribution,  $\Pi_o(p)$ , can be read off directly from (31):

$$\Pi_{o(a+b+c)}(p) = \frac{g^4 B}{16\pi^2} \left(1 + \frac{\pi^2}{4}\right) \frac{1}{N}. \quad (63)$$

Calculating the even contribution,  $\Pi_e(p)$ , however, is much more complicated. In addition to the cumbersome Dirac trace, the evaluation of the Feynman integrals are highly non-trivial. We leave the details to an appendix and here only quote the final result,

$$\Pi_e(p) \approx -\frac{3A}{16} \frac{g^4}{(2\pi)^2} \frac{1}{N}. \quad (64)$$

It should be emphasized that all divergent contributions to the polarization tensor  $\Pi_{\mu\nu}(p)$  cancel, so that in the  $1/N$  expansion the  $\beta$ -function  $\beta(g)$  vanishes, and conformal invariance survives quantum fluctuations at the transition point.

Finally we can obtain the Fermion conductivities at the critical point from the above polarization tensors. Eq. (13) can be used to obtain the conductivity per flavor of massless Dirac field. To obtain the total Fermion conductivity per flavor we must add to  $\sigma_{F,xy}$  the

contribution of  $-1/2$  from the massive Dirac field. The final result to leading order in  $1/N$  is:

$$\sigma_{F,xy} = -\frac{1}{2} + 16\left(1 + \frac{\pi^2}{4}\right) \frac{\alpha}{64 + (\pi\alpha)^2} \frac{1}{N}, \quad (65)$$

$$\sigma_{F,xx} \approx \frac{\pi}{8} \left(1 + \frac{12\alpha^2}{64 + (\pi\alpha)^2} \frac{1}{N}\right). \quad (66)$$

#### IV. DISCUSSION

As we have seen, the critical properties of the Mott anyon transition vary continuously with the anyon statistics. Thus the model describes a line of fixed points which are characterized by the statistics parameter  $\alpha$ , which varies from Fermions,  $\alpha = 0$ , to Bosons,  $\alpha = 1$ . In Section III we calculated the critical exponents and universal conductivities at the anyon Mott transition as an expansion around the Fermion point. Specifically, in terms of the deviation from Fermi statistics,  $\alpha$ , we obtained critical exponents up to second order and conductivities to first order. The critical properties at the Mott transition can also be obtained at  $\alpha = 1$  directly in terms of a Bosonic scalar (U(1)) field theory, or equivalently the 3D XY model [11]. The exponents are of course known quite accurately for the 3D XY model, and recently an estimate for the conductivity has been obtained from Monte Carlo simulations and a large N expansion [12]. Also, within a large N calculation Wen and Wu [13] have recently performed an expansion for  $\alpha$  near one by coupling a Chern-Simons gauge-field to the U(1) Boson field. It is instructive to compare these various results for the critical properties of the Mott transition in order to see the trends in exponents and conductivities as one varies the particle statistics from Fermi to Bose. As we discuss below, the observed trend can give one some insight into possible connections between transitions in the integer quantum Hall effect [35], and the magnetic field-tuned superconductor insulator transition in thin films [36], [37].

Consider first the exponents  $\eta$  and  $\nu$ . In Section III we found that to second order in  $\alpha$ ,

$$\eta(\alpha) = 1 - \frac{1}{3}\alpha^2 + O(\alpha^3), \quad \nu^{-1}(\alpha) = 1 + \frac{17}{6}\alpha^2 + O(\alpha^3). \quad (67)$$

For the 3D XY model, which corresponds to  $\alpha = 1$ , the exponents are given by roughly,

$$\eta(\alpha = 1) \sim 1/50, \quad \nu^{-1}(\alpha = 1) \sim 3/2. \quad (68)$$

Notice that both  $\eta$  and  $\nu$  are smaller for Bosons than for Fermions. Moreover, the expansion from the Fermion end indicates that the initial deviations for small  $\alpha$  are to reduce the exponents, suggesting that  $\eta(\alpha)$  and  $\nu(\alpha)$  might be monotonically decreasing functions of  $\alpha$ . Unfortunately, as is clear from this expansion, the leading order term does not give a reliable estimate at  $\alpha = 1$ . This should be contrasted with the  $\epsilon = 4 - D$  expansion for the XY model [38] which gives reasonable exponent values for the 3D model when the low order results are extrapolated to  $\epsilon = 1$ .

It is also instructive to compare the 3D XY exponents with the exponents obtained from the large N Fermion expansion in Section 3:

$$\eta = 1 - \frac{8}{3} \frac{\alpha^2}{64 + (\pi\alpha)^2} \frac{1}{N}, \quad (69)$$

$$\nu^{-1} = 1 + \frac{128}{3} \frac{(128 - (\pi\alpha)^2)\alpha^2}{(64 + (\pi\alpha)^2)^2} \frac{1}{N}. \quad (70)$$

If we put  $\alpha = 1$  these become

$$\eta(\alpha = 1) = 1 - (0.036\dots)(1/N) + O(1/N^2), \quad (71)$$

$$\nu^{-1}(\alpha = 1) = 1 + (0.924\dots)(1/N) + O(1/N^2), \quad (72)$$

which, when extrapolated to  $N=1$ , should become equal to the 3D XY model exponents. Once again, although the leading term in the expansion has the ‘correct’ sign, the extrapolations to  $N=1$  using only the first term are clearly not very reliable.

Next we consider the universal conductivities at the Mott transition. For Fermions,  $\alpha = 0$ , we obtained in Section III that  $\sigma_{xx} = \pi/8$  and  $\sigma_{xy} = -1/2$ . For the Boson Mott transition (in zero field)  $\sigma_{xy} = 0$  and the recent numerical estimates [12] give  $\sigma_{xx}(\alpha = 1) = 0.285 \pm 0.02$ , a value slightly smaller than in the Fermion case. It is instructive to see if the expansion about the Fermion point for small  $\alpha$  gives the correct trends. For this purpose it is both more natural and easier to compare resistivities, since as (14) shows the longitudinal anyon resistivity is simply equal to the Fermion longitudinal resistivity. Upon inverting the

perturbative results in Equation (32) and (33) for the Fermion conductivity, we obtain, using (14), an expansion for the anyon longitudinal resistivity:

$$\rho_{xx}(\alpha) = (0.9715\dots) + (2.084\dots)\alpha + O(\alpha^2) . \quad (73)$$

Similarly, the transverse anyon resistivity is given by:

$$\rho_{xy}(\alpha) = (1.237\dots) - (0.492\dots)\alpha + O(\alpha^2) . \quad (74)$$

The universal resistivities at  $\alpha = 1$  follow from the Boson Monte Carlo simulations and are [12]

$$\rho_{xx}(\alpha = 1) = 3.5 \pm 0.2 , \quad \rho_{xy}(\alpha = 1) = 0 . \quad (75)$$

Notice that the sign of the leading small  $\alpha$  correction to both  $\rho_{xx}$  and  $\rho_{xy}$  are such that the values tend towards the boson values in (75). This result suggests that, just as with the critical exponents, the components of the universal resistivity tensor vary monotonically upon moving along the fixed line of critical points from Fermion to Boson statistics.

One might be tempted to compare directly our large- $N$  results to those obtained in Ref. [13] for  $N$ -flavors of Bosons coupled to the Chern-Simons field. However, the two large  $N$ -theories are probably not continuously connected to one another (upon varying  $\alpha$ ) since the extension to  $N$  fields brings into the Lagrangian of the theory a new  $SU(N)$  symmetry, which is spontaneously broken upon crossing the Bosonic transition, while unaffected across the Fermionic phase transition.

We now turn to the relevance of the results obtained in this paper to two-dimensional experimental systems which exhibit zero temperature quantum phase transitions. Unfortunately we cannot make direct contact with experiment, since our simplified lattice model ignores both disorder and long-ranged Coulomb interactions. Nevertheless, the notion of a fixed line of critical points parameterized by the statistics of the underlying particles, along which the exponents vary continuously, and monotonically, is presumably rather more general.

To be specific, consider a more realistic model of anyons, with a long-ranged Coulomb interaction moving in a quenched random potential and external magnetic field. In the Boson limit,  $\alpha = 1$ , as parameters are varied this model presumably undergoes a transition from a superconducting phase to a localized Bose glass insulator. This transition is believed to be in the appropriate universality class for real disordered superconducting films, which are tuned with an external magnetic field from the superconducting into insulating phases [37]. This magnetic field tuned superconductor-insulator transition has been recently studied experimentally in considerable detail [36]. In the Fermion limit,  $\alpha = 0$ , with strong disorder the model is presumed to exhibit transitions between integer quantum Hall plateaus, for which there is also considerable experimental data [35]. The critical properties of these two experimentally accessible phase transitions are thus presumably end points of a fixed line of critical points which interpolates between them. Moreover, transitions between fractional plateaus in the quantum Hall effect are probably described correctly by this same model with fractional statistics  $\alpha$ . For example, the transition between the so-called Hall insulator and the  $\nu = 1/3$  quantum Hall plateau can be described as a condensation of fractional statistics particles with  $\alpha = 2/3$ .

Although at present we cannot calculate analytically (or numerically) the critical properties along the fixed line of these disordered anyon models, it is instructive to compare the critical properties measured experimentally with the trends obtained in our simplified clean lattice model. For example, experiments [35] on the transition between integer plateaus in the Hall effect find that the correlation length exponent,  $\nu$ , times the dynamical exponent,  $z$ , to be given by roughly  $7/3$ . Since one expects  $z=1$  in the presence of  $1/r$  Coulomb interactions [18], this gives an estimate for  $\nu \sim 7/3$ . At the magnetic field tuned superconductor insulator transition, on the other hand, with  $z=1$  assumed, the experiments give a much smaller value,  $\nu \sim 5/4$ . Thus upon moving along the presumed line of fixed points from the Fermion to Boson end, the exponent  $\nu$  apparently decreases. It is noteworthy that this same trend, a decreasing of  $\nu$  moving from Fermion to Boson, was what we found along the fixed line of Mott anyon transitions. Perhaps it is generic that Fermion transitions are closer to



their lower critical dimension, with a larger  $\nu$ , than their Boson counterparts.

It is also amusing to compare the experimental values for the universal resistivities at the two transitions. At the field tuned superconductor-insulator transition [36] the longitudinal resistivity is found to cluster in the range between 0.8 and 1.0, in units of  $h/(2e)^2$ , where the Cooper pair has charge  $2e$ . At the transition between integer plateaus in the quantum Hall effect, experiments find [39] values of  $\sigma_{xx}$  of roughly 0.2. Combining this with  $\sigma_{xy} = 1/2$  gives  $\rho_{xx}$  of roughly 0.7, a value slightly smaller than at the superconductor-insulator transition. It is interesting that at the anyon Mott transition we also find the longitudinal resistivity increases moving from the Fermion to Boson end. It is of course unclear whether or not this trend is a generic property of anyon phase transitions.

Finally, it is worth re-emphasizing that the existence of a fixed line of critical points characterized by the anyon statistics in our simple lattice anyon model, underscores the importance of the fluctuating gauge field. At a critical point, or more generally in a gapless phase, the fluctuating Chern-Simons gauge field cannot be simply thrown away, as in the ‘flux-smearing’ mean field approaches. More specifically, we expect that the presence of this fluctuating gauge field will most likely make the transition between plateaus in the fractional quantum Hall effect in a different universality class from that between integer plateaus.

#### ACKNOWLEDGMENTS

W.C. thanks I. Affleck and G.W. Semenoff for discussions. M.P.A.F. is extremely grateful to Nick Read and R. Shankar for numerous clarifying conversations during the formative part of this work, and to the Institute for Theoretical Physics in Santa Barbara where part of this work was initiated. Y.S.W. thanks X.G. Wen for helpful discussions, and R.A. Webb and D.H. Lee for warm hospitality at IBM, and R. Jackiw and X.G. Wen for warm hospitality at MIT. This work was supported in part by the Natural Sciences and Engineering Research Council of Canada and U.S. National Science Foundation through grant No. PHY-9008452 and by the National Science Foundation under grant No. Phy89-04035.

#### APPENDIX: Calculation of $\Pi_e(p)$ at order $\mathcal{O}(1/N)$

In this appendix we present the details for the two-loop calculation of the even part of

the gauge-boson self-energy  $\Pi_e(p)$  in the  $1/N$  expansion.

Some useful formula for the  $2 \times 2$   $\gamma$ -matrices are

$$\mathbf{Tr}(\gamma^\mu \gamma^\nu \gamma^\lambda \gamma^\sigma) = 2(\delta^{\mu\nu} \delta^{\lambda\sigma} + \delta^{\mu\sigma} \delta^{\nu\lambda} - \delta^{\mu\lambda} \delta^{\nu\sigma}), \quad (76)$$

$$\mathbf{Tr}(\gamma^\mu \gamma^\nu \gamma^\lambda) = 2\epsilon^{\mu\nu\lambda}, \quad (77)$$

$$\gamma^\mu \gamma^\mu = -3 \cdot \mathbf{1}, \quad (78)$$

$$\gamma^\mu \gamma^\lambda \gamma^\mu = \gamma^\lambda, \quad (79)$$

$$\gamma^\mu \gamma^\sigma \gamma^\lambda \gamma^\mu = 2\delta^{\sigma\lambda} \mathbf{1} - \gamma^\lambda \gamma^\sigma, \quad (80)$$

$$\not{k} \not{k} = -k^2 \mathbf{1}, \quad (81)$$

$$\gamma^\mu \gamma^\nu \gamma^\rho \epsilon^{\nu\mu\tau} p^\tau = 2p^\nu \mathbf{1}. \quad (82)$$

The relevant diagrams are those in Fig. 11. Note that  $\Pi_e = \frac{1}{2p} \delta^{\mu\nu} \Pi^{\mu\nu}$ . We have  $\Pi_e^{(a+b)}$  and  $\Pi_e^{(c)}$  are therefore given by

$$\begin{aligned} & -\frac{A g^4}{p N} \mu^{6-D'-D} \int \frac{d^{D'} k}{(2\pi)^{D'}} \frac{d^D q}{(2\pi)^D} \mathbf{Tr} \frac{\gamma^\mu (\not{k} + \not{p}) \gamma^\mu \not{k} \gamma^\nu (\not{k} + \not{q}) \gamma^\sigma \not{k} (\delta^{\sigma\nu} q^2 - q^\sigma q^\nu)}{k^4 (k+p)^2 (k+q)^2 q^3} \\ & = -4 \frac{A g^4}{p N} \mu^{6-D'-D} \int \frac{d^{D'} k}{(2\pi)^{D'}} \frac{d^D q}{(2\pi)^D} \frac{q \cdot (q+k) (2k \cdot pk \cdot q + k^2 k \cdot q - k^2 p \cdot q)}{k^4 (k+p)^2 (k+q)^2 q^3} \end{aligned} \quad (83)$$

and

$$\begin{aligned} & -\frac{A g^4}{p 2N} \mu^{6-D'-D} \int \frac{d^{D'} k}{(2\pi)^{D'}} \frac{d^D q}{(2\pi)^D} \mathbf{Tr} \frac{\gamma^\mu (\not{k} + \not{p}) \gamma^\nu (\not{k} + \not{q} + \not{p}) \gamma^\mu (\not{k} + \not{q}) \gamma^\sigma \not{k} (\delta^{\sigma\nu} q^2 - q^\sigma q^\nu)}{k^2 (k+p)^2 (k+q)^2 (k+q+p)^2 q^3} \\ & = -2 \frac{A g^4}{p N} \mu^{6-D'-D} \int \frac{d^{D'} k}{(2\pi)^{D'}} \frac{d^D q}{(2\pi)^D} \frac{G(k, q, p)}{k^2 (k+p)^2 (k+q)^2 (k+q+p)^2 q^3}, \end{aligned} \quad (84)$$

respectively, where

$$\begin{aligned} G(k, q, p) & = k^2 [q^4 - q^2 p \cdot q - 2q^2 k \cdot q - 2q^2 k \cdot p - (q \cdot p)^2 + q^2 p^2 - k^2 q^2] \\ & + (k \cdot q) [-2q^2 k \cdot q + 2(q \cdot p)(k \cdot p) - 2q^2 k \cdot p - 2q^2 q \cdot p - p^2 k \cdot q] \\ & + q^2 (k \cdot p) [q^2 - q \cdot p - 2k \cdot p]. \end{aligned} \quad (85)$$

Performing the convergent  $k$ -integrations in Eqs. (83, 84) at  $D' = 3$ , we have

$$\Pi_{e(a+b)} = \frac{A}{p} \frac{g^4}{8N} \mu^{3-D} \int \frac{d^D q}{(2\pi)^D} \left[ \frac{2q \cdot p + p^2}{q^3 |q+p|} - \frac{q \cdot p}{q^2 |q+p| p} \right]. \quad (86)$$

$$\Pi_{e(c)} = -\frac{A}{p} \frac{g^4}{8N} \mu^{3-D} \int \frac{d^D q}{(2\pi)^D} \left[ \frac{2q \cdot p + p^2}{q^3 |q+p|} + \frac{4p}{q^2 |q+p|} + \frac{1}{q |q+p|} + \frac{2q^4 + 5p^2 q^2 + 2p^4}{(q \cdot p) q^2 |q+p| p} \right]. \quad (87)$$

Due to the factor  $q \cdot p$  in the denominator of the last term in (87), it is hard to obtain an analytic expression with the dimensional regularization. So we will set  $D = 3$  and introduce a momentum cut-off  $\Lambda$  in both (86) and (87). We will see the logarithmically divergent terms indeed cancel. Also we will discard linearly divergent terms, whose appearance is an artifact of this regularization by momentum-cut-off. (Such divergences do not appear in a regularization that preserves Lorentz invariance.) This results in a finite contribution to  $\Pi_e$  at the order  $\mathcal{O}(1/N)$ :

$$\Pi_{e(a+b+c)} = -\frac{A}{p} \frac{g^4}{8N} \int^\Lambda \frac{d^3 q}{(2\pi)^3} \left[ \frac{q \cdot p}{q^2 |q+p| p} + \frac{4p}{q^2 |q+p|} + \frac{1}{q |q+p|} + \frac{2q^4 + 5p^2 q^2 + 2p^4}{(q \cdot p) q^2 |q+p| p} \right]. \quad (88)$$

Except for a factor  $-\frac{A}{8N} \frac{g^4}{(2\pi)^2}$ , the first three terms are, respectively,

$$-\frac{2}{9} - \frac{1}{3} \ln \frac{\Lambda^2}{p^2}, \quad 8 + 4 \ln \frac{\Lambda^2}{p^2}, \quad -2. \quad (89)$$

The fourth term is a bit messy:

$$\begin{aligned} & \frac{1}{2} \int_0^1 dy \frac{2 + 5y + 2y^2}{y \sqrt{1+y}} \ln \frac{\sqrt{1+y} - \sqrt{y}}{\sqrt{1+y} + \sqrt{y}} + \frac{1}{2} \int_1^{\frac{\Lambda^2}{p^2}} dy \frac{2 + 5y + 2y^2}{y \sqrt{1+y}} \ln \frac{\sqrt{1+y} - 1}{\sqrt{1+y} + 1} \\ &= \frac{1}{2} \int_0^1 dy \frac{2 + 5y + 2y^2}{y \sqrt{1+y}} \ln \frac{\sqrt{1+y} - \sqrt{y}}{\sqrt{1+y} + \sqrt{y}} + C - \frac{22}{6} \ln \frac{\Lambda^2}{p^2}. \end{aligned} \quad (90)$$

where

$$C = -\frac{64}{9} - \frac{1}{2} \left[ \ln \frac{\sqrt{2} + 1}{\sqrt{2} - 1} \right]^2 + \frac{13\sqrt{2}}{3} \ln \frac{\sqrt{2} + 1}{\sqrt{2} - 1} = 2.137820914. \quad (91)$$

The integral in (90) is numerically evaluated to be  $-6.405956452 \dots$ . The logarithmic divergences cancel out and the final finite result is

$$\Pi_e(p) = -1.509642238 \frac{A}{8N} \frac{g^4}{(2\pi)^2} \approx -\frac{3A}{16N} \frac{g^4}{(2\pi)^2}. \quad (92)$$

## REFERENCES

- [1] F. Wilczek, Phys. Rev. Lett. **48**, 1144 (1982); Phys. Rev. Lett. **49** 957 (1982); Y.S. Wu, Phys. Rev. Lett. **53**, 111 (1984).
- [2] A. Fetter, C. Hanna and R. Laughlin, Phys. Rev. **B39** (1989) 9679.
- [3] S.M. Girvin and A.H. Macdonald, Phys. Rev. Lett. **58** 1252 (1987).
- [4] S.C. Zhang, T.H. Hansen and S. Kivelson, Phys. Rev. Lett. **62**, 82 (1989); D.H. Lee and S.C. Zhang, Phys. Rev. Lett. **66**, 1220 (1991).
- [5] N. Read, Phys. Rev. Lett. **62**, 86 (1989).
- [6] J.K. Jain, Phys. Rev. Lett. **63** (1989) 199; Phys. Rev. **B40** (1990) 8079.
- [7] B. Blok and X.G. Wen, Phys. Rev. **B42** (1990) 8133; X.G. Wen and A. Zee, Nucl. Phys. **B351** (1990) 135; X.G. Wen, Mod. Phys. Lett. **B5** (1991) 39.
- [8] B.I. Halperin, P.A. Lee and N. Read, preprint, 1992.
- [9] D.H. Lee, S. Kivelson and S.C. Zhang, Phys. Rev. Lett. **68**, 2389 (1992); preprint, 1992.
- [10] G.S. Canright, S.M. Girvin and A. Brass, Phys. Rev. Lett. **63**, 2295 (1989).
- [11] M.P.A. Fisher, P.B. Weichman, G. Grinstein and D.S. Fisher, Phys. Rev **B40**, 546 (1989).
- [12] M. Cha, M.P.A. Fisher, S.M. Girvin, M. Wallin and A.P. Young, Phys. Rev **B44**, 6883 (1991).
- [13] X.G. Wen and Y.-S. Wu, MIT preprint (July, 1992).
- [14] A tight binding model with half of a flux quantum per plaquette arises in ‘flux-phase’ mean field treatments of frustrated two-dimensional antiferromagnets. See, for example, X.G. Wen et. al. Phys Rev. **B39**, 11413 (1989).

- [15] D.J. Thouless, M. Kohmoto, N.P. Nightingale and M. den Nijs, Phys. Rev. Lett. **49**, 405 (1982).
- [16] We are grateful to R. Shankar for the following particularly succinct derivation of the final Dirac representation in Equation (7).
- [17] W. Siegel. Nucl. Phys. **B156** (1979) 135; J.J. Schonfeld, Nucl.Phys. **B185** (1981) 157; R. Jackiw and S. Templeton, Phys. Rev. **D32** (1981) 2291.
- [18] M.P.A. Fisher, G. Grinstein and S.M. Girvin, Phys. Rev. Lett. **64**, 587 (1990); X.G. Wen and A. Zee, Int. J. Mod. Phys.B **4**, 437 (1990).
- [19] D. Amit, *Field Theory, Renormalization Group and Critical Phenomena*,(Second Edition), World Scientific, 1988.
- [20] G. Parisi, *Statistical Field Theory*, Addison-Wesley, 1988.
- [21] P. Ramond, *A Primer of Field Theory*, Addison-Wesley, 1988.
- [22] S. Deser, R. Jackiw and S. Templeton, Phys. Rev. Lett. **48** (1982) 975; Ann. Phys. (N.Y.) **140** (1982) 372.
- [23] S. Coleman and B. Hill, Phys. Lett. **159B** (1985) 184.
- [24] N. Redlich, Phys. Rev. **D29** (1984) 2366.
- [25] A. Niemi, G.W. Semenoff and Y.-S. Wu, Nucl. Phys. **B276** (1986) 173.
- [26] G.W. Semenoff, P. Sodano and Y.-S. Wu, Phys. Rev. Lett. **62** (1989) 715.
- [27] W. Chen, G.W. Semenoff and Y.-S. Wu, Mod. Phys. Lett. **A5** (1990) 1833; in *Physics, Geometry and Topology*, Proc. of Banff Summer School on Particles and Fields, August 1989; (Plenum Pub. Cor.), p.553, 1990.
- [28] W. Chen, G.W. Semenoff and Y.-S. Wu, Phys. Rev. **D44** (1991) R1625; and Phys. Rev. D, in press.

- [29] W. Chen, Phys. Lett. **251B** (1990) 415.
- [30] W. Chen (unpublished) (1990).
- [31] V.P. Spiridonov and F.V. Tkachov, Phys. Lett. **B260** (1991) 109.
- [32] There is a huge literature for perturbative calculation of the induced Chern-Simons term in various  $D = 2 + 1$  quantum field theories other than Abelian Chern-Simons coupled to non-self-interacting matter. An incomplete list is: Y. Kao and M. Suzuki, Phys. rev. **D31** (1985) 2137; M. Bernstien and T.J. Lee, Phys. Rev. **D32** (1985) 1020; R. Pisarski and S. Rao, Phys. Rev. **D32** (1985) 2081; T. Lee, Phys. Lett. 171B (1986) 247; V.P. Spidonov, JETP Lett. **52** (1990) 1112; L.V. Avdeev, G.V. Grigoriev and D.I. Kazakov, CERN preprint TH-6091/91 (1991); G. Ferretti and S.G. Rajeev, Mod. Phys. Lett. bf A7 (1992) 2087; S.H. Park, Phys. Rev. **D45** (1992) R3332; D.K. Hong, T. Lee and S.H. Park, Korea preprint SNUTP 92/91 (1992); J. Chay, D.K. Hong, T. Lee and S.H. Park, Korea preprint SNUTP 92/92 (1992).
- [33] In fact the beta-function  $\beta(g)$  vanishes by explicit calculation at two loops even in non-Abelian theory [28]; it is proved to vanish up to all orders in perturbation theory in massive Dirac theory, and is conjectured to do so in massless theory. An argument for the latter case can be given as follows: The Chern-Simons Lagrangian is gauge invariant only up to total divergence terms. But on the other hand, only strictly gauge invariant local counterterms can arise in a gauge-invariant regularization and renormalization scheme. So no infinite counterterm for the Chern-Simons Lagrangian can appear.
- [34] The divergence of the pole  $2/\epsilon \equiv 2/(3-D)$  in the physical dimension  $D = 3$  corresponds to  $\ln(\Lambda^2/\mu^2)$  in the regularization with momentum cutoff  $\Lambda$ .
- [35] H.P. Wei, D.C. Tsui, M.A. Paalanen and A.M.M. Pruisken, Phys. Rev. Lett. **61**, 1294 (1988).
- [36] A.F. Hebard and M.A. Paalanen, Phys. Rev. Lett. **65**, 927 (1990).

[37] M.P.A. Fisher, Phys. Rev. Lett. **65**, 923 (1990).

[38] M.E. Fisher, Rev. Mod. Phys. **46**, 597 (1974).

[39] D.C. Tsui (private communication).

FIGURES

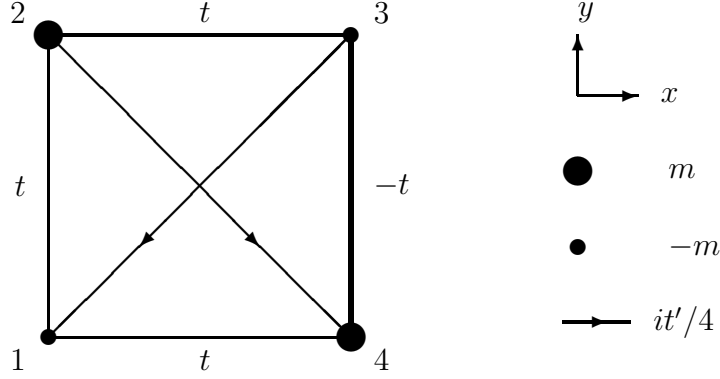


**Fig. 1** The four sites in the unit cell of the two-dimensional square lattice tight binding model with one-half of a flux quanta per plaquette and a staggered periodic potential. Near neighbors have hopping strength  $t$  except the bold line which is  $-t$ . The next-near neighbors have a hopping strength  $it'/4$ , and the staggered on-site potential has strength  $m$ .

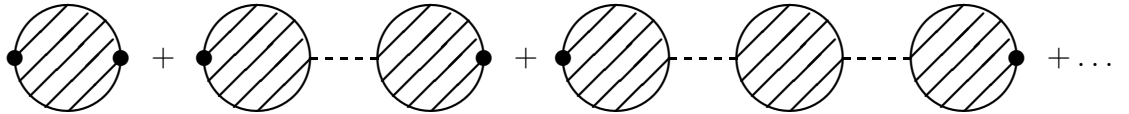


**Fig. 2** The full current-current correlation for the external electromagnetic field. The black spots stand for the currents. The striped disk represents the exact Chern-Simons self-energy and the dashed line the Chern-Simons propagator.





**Fig. 3** (a) Chern-Simons and (b) fermion self-energies at  $\mathcal{O}(e^2)$ . The solid line stands for the fermion propagator.

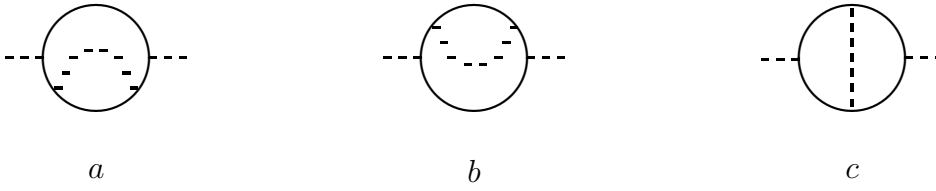


**Fig. 4** Chern-Simons self-energy at  $\mathcal{O}(e^4)$ .

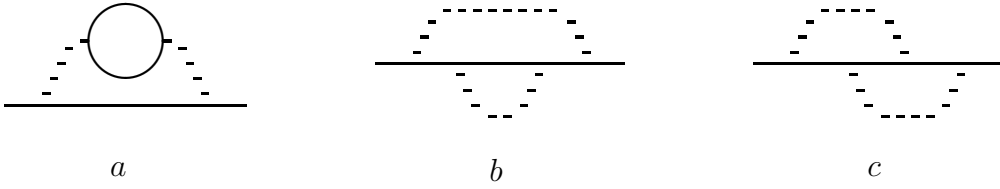


**Fig. 5** Fermion self-energy at  $\mathcal{O}(e^4)$ .

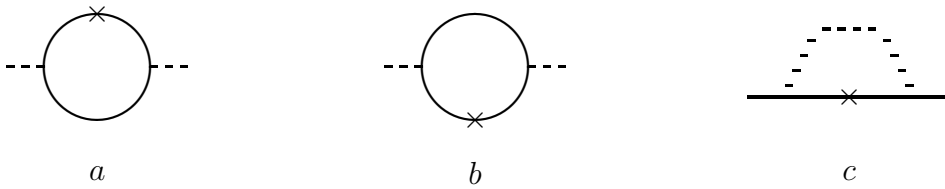


**Fig. 6** Vertices with composite operator insertions at  $\mathcal{O}(e^2)$ . The cross stands for the composite operator  $\bar{\psi}\psi$ .

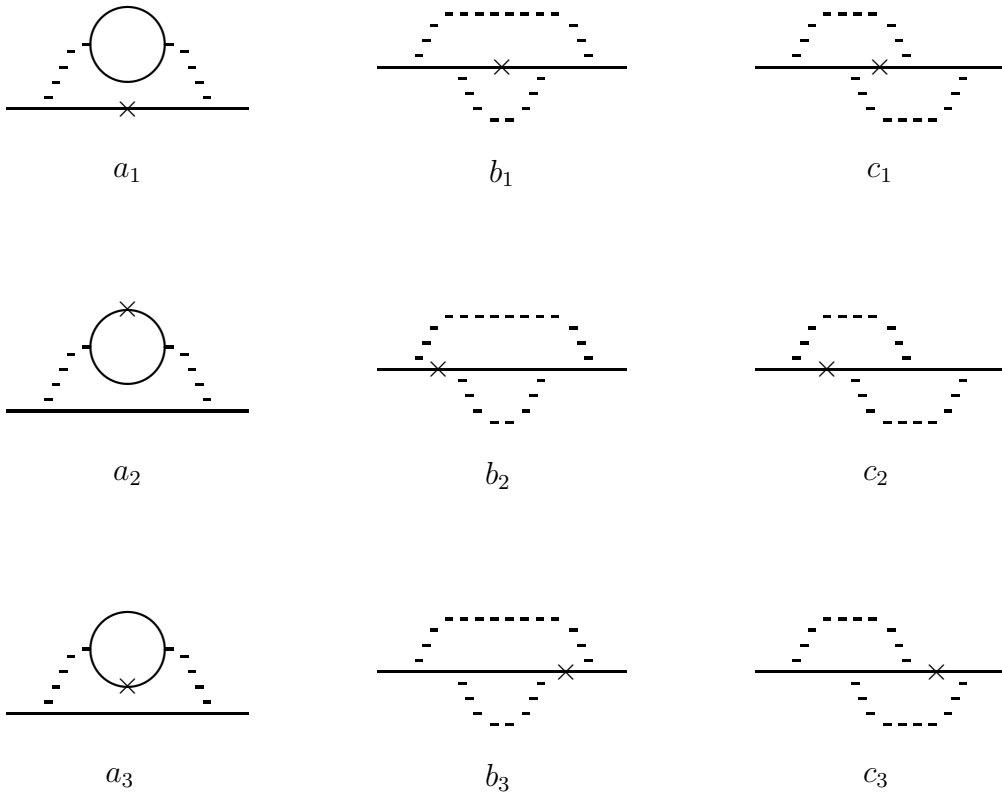


**Fig. 7** Fermion vertex with the insertion of the composite operator  $\bar{\psi}\psi$  at  $\mathcal{O}(e^4)$ .

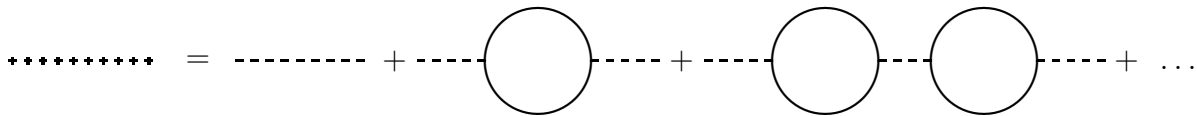


**Fig. 8** Summation of infinite series of one-loop Fermion bubble chains gives the dressed Chern-Simons propagator, which is of order  $\mathcal{O}(N^0)$ . The cross line is the dressed Chern-Simons propagator, the solid lines are the Fermion propagators, the dashed lines are the bare Chern-Simons propagators.



**Fig. 9** Fermion self-energy at  $\mathcal{O}(1/N)$ .

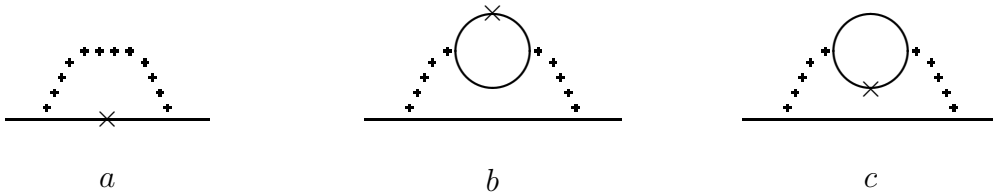


**Fig. 10** Fermion vertex with an insertion of the composite operator  $\bar{\psi}_i\psi_i$  at  $\mathcal{O}(1/N)$ .

The cross stands for the composite operator  $\bar{\psi}_i\psi_i$ .

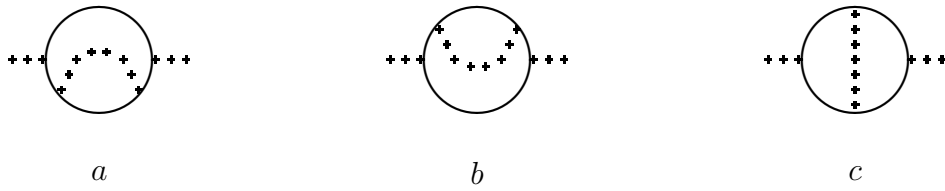


**Fig. 11** Chern-Simon self-energy at  $\mathcal{O}(1/N)$ .

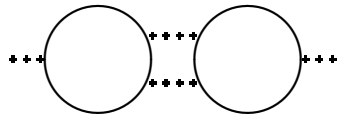


**Fig. 12** Null diagram at order  $\mathcal{O}(1/N)$ .